REGIME VARIANCE TESTING — A QUANTILE APPROACH*

Janusz Gajda, Grzegorz Sikora, Agnieszka Wyłomańska

Hugo Steinhaus Center, Institute of Mathematics and Computer Science
Wrocław University of Technology
Janiszewskiego 14a, Wrocław 50-370, Poland

(Received May 10, 2013)

In this paper, we examine time series that exhibit behavior related to two or more regimes with different statistical properties. The motivation of our study are two real data sets from plasma physics with an observable two-regimes structure. In this paper, we develop a procedure to estimate the critical point of the division in a structural change in a time series. Moreover, we propose three tests to recognize such specific behavior. The presented methodology is based on the empirical second moment and its main advantage is the assumption of a lack of distribution. Moreover, the examined statistical properties are expressed in the language of empirical quantiles of the squared data, therefore, the methodology is an extension of the approach known from the literature. Theoretical results are confirmed by simulations and analysis of real data of turbulent laboratory plasma.

DOI:10.5506/APhysPolB.44.1015
PACS numbers: 02.70.–c, 02.50.–r, 05.40.–a

1. Introduction

The main issue in real data analysis is testing distribution. This problem appears not only in the case of an independent identically distributed (i.i.d.) sample [1–3] but also when we calibrate a model to a real data set [4–6]. In this case, the distribution is fitted to the residual series that is assumed to be i.i.d. But many independent variables seem to display changes in the underlying data generating process over time [7], therefore, they cannot be considered as an identically distributed sample. This typical behavior is also observed in time series described in Sec. 2 that presents increments of floating potential fluctuations of turbulent laboratory plasma for the small torus radial position $r = 9.7$ cm. For this data set, known statistical tests for

* Presented at the XXV Marian Smoluchowski Symposium on Statistical Physics, "Fluctuation Relations in Nonequilibrium Regime", Kraków, Poland, September 10–13, 2012.

the stationarity, mentioned in Sec. 3 [8–12], are not useful. What is more, under some assumptions they indicate the data are i.i.d. that is contradictory to the behavior of the data observable in Fig. 1.

In this paper, we introduce three tests that can be useful for time series for which we observe more than one regime with different statistical properties. Two of them are visual, therefore, we call them pre-tests and propose to use them in the preliminary analysis to identify the specific behavior. In order to confirm two or more regimes in the data set, we have developed a statistical test for regime variance. Moreover, we also introduce the estimation procedure for the critical point that divides an examined time series into two parts with different statistical properties. However, only an inspection of the data can sometimes lead to the wrong preliminary choice of the model, therefore, the aforementioned tests are based on the behavior of the empirical second moment of the examined time series. This approach was also considered in [13] for testing the behavior of two-regimes. The advantage of this methodology based on the empirical moments is emphasized in [14, 15] and is also confirmed by the bottom panel of Fig. 1 which presents the squared data for which the difference between two regimes is more visible. In contrast to [13], where authors assume the Gaussian distribution of the examined time series, in the presented methodology we do not assume the distribution of a given series because the introduced tests exploit only the empirical properties of the examined data set. More importantly, they can be used for data for which the point of division into two regimes is well-defined (is clearly observable), but also for data for which the point is not visible. Moreover, we show by simulation study that the proposed methodology can also be useful for an infinite-variance time series.

The rest of the paper is organized as follows: in Sec. 2, we present the examined data sets that are the motivation of developing the presented methodology. In Sec. 3, we overview the known statistical tests for stationarity and present the estimation procedure to recognize the critical point introduced in [16]. In Sec. 4, we introduce two visual pre-tests that indicate the specific behavior of an examined time series, *i.e.* two regimes related to different statistical properties. In this section, we also propose an innovative procedure to estimate the critical point based on the behavior of an empirical second moment of real data set and present the simulation study. The estimation procedure can be useful not only for data with the Gaussian distribution, therefore, we extend the methodology presented in [13], where authors assume the normal behavior of an examined time series. In Sec. 5, we introduce the statistical method for testing regime variance and test the procedure by using simulated data. In the next section, we analyze real data sets from plasma physics using the presented methodology. Finally, the last section gives few concluding remarks.

2. Motivation

The motivation of our study is presented in Fig. 1 real data set. This time series describes increments of floating potential fluctuations (in volts) of turbulent laboratory plasma for the small torus radial position $r = 9.7$ cm. A precise description of the experiment is presented in [17]. The similar data sets from plasma physics were also examined in [14]. The signal was registered on June 15, 2006 with movable probe in scrape-off layer (SOL) plasma of stellarator "URAGAN 3M". Because the signal was registered every 0.0000016 seconds, the total length of the time series is 30 000, but for the analysis we only took 1900 observations between 12 000–13 900.

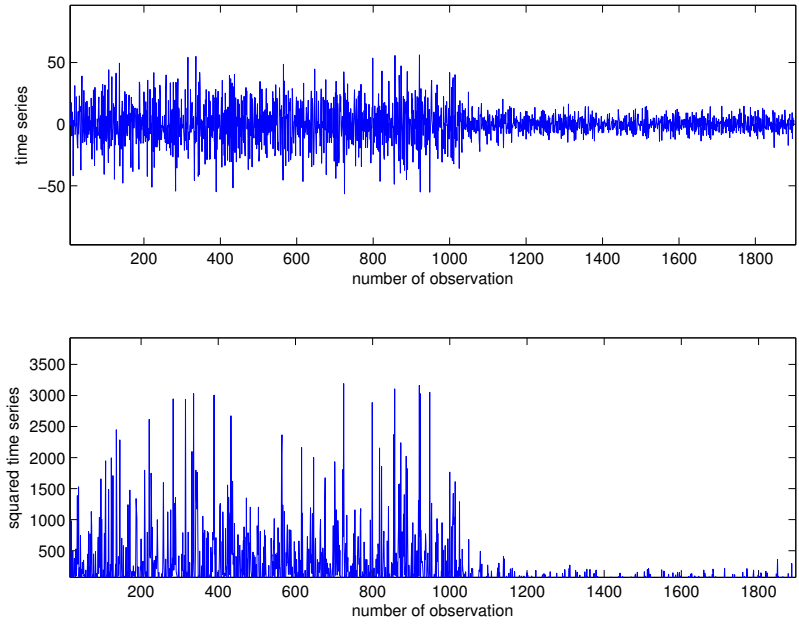

Fig. 1. The empirical time series from plasma physics that presents increments of floating potential fluctuations (in volts) of turbulent laboratory plasma for the small torus radial position $r = 9.7$ cm (top panel) and squared time series (bottom panel).

As can be observed in Fig. 1, the empirical data set exhibits very special behavior, namely the statistical properties of the time series change in time. From the physical point of view, it is related to the so-called L–H transition phenomenon, that is a sudden transition from a low confinement mode (L mode) to a high confinement mode (H mode), accompanied by suppression of turbulence and a rapid drop of turbulent transport at the edge of thermonuclear device [14, 18]. From the mathematical point of view, this

special behavior can be related to the fact that the first observations constitute a random sample that comes from another distribution, than the last part or those two parts come from the same distribution with different parameters. Therefore, we can suspect that the time series satisfies the following property

$$X_i \stackrel{d}{=} \begin{cases} X & \text{for} \quad i \leq l\,, \\ \\ Y & \text{for} \quad i > l\,, \end{cases} \tag{1}$$

where X and Y are independent and have different statistical properties, and l is a fixed point. As we have mentioned in Sec. 1, inspection of the data can sometimes lead to wrong preliminary conclusions, therefore, we propose to consider the squared time series. As can be observed in Fig. 1, the difference between two parts is more visible for squared data (bottom panel of Fig. 1). The statistical properties are expressed in the language of quantiles of a squared time series and we assume the random variables X^2 and Y^2 in relation (1) have different quantiles $q_{\alpha/2}$ and $q_{1-\alpha/2}$ for given confidence level α. Here we take notation q_a as a quantile of the order of a.

After preliminary analysis of the data set and confirmation that it constitutes realizations of independent random variables (see Fig. 11), the hypothesis of the same distribution of the time series was tested. The known statistical tests such as Augmented Dickey–Fuller, Phillips–Perron or Kwiatkowski–Phillips–Schmidt–Shin test for stationarity reject the hypothesis that the data are nonstationary (in the sense presented in Sec. 3), which suggests they are not useful for this data set. Therefore, we propose three tests that can be used for data that exhibit similar behavior as observed in Fig. 1, but also to this that after preliminary analysis we cannot reject the hypothesis about the same distribution. An example is shown in Fig. 2. This time series presents increments of floating potential fluctuations (in volts) of turbulent laboratory plasma for the small torus radial position $r = 9.8$ cm. Similar to the first data set, the signal was registered on June 15, 2006 and the total number of observations was 30 000 but to illustration only observations from 12 000 to 15 000 were taken. After analysis of the time plot for the series and squared series, we can suspect that the data cannot be considered as an identically distributed sample but here, when some statistical properties change is not as visible as for the first data set. Moreover, the tests for stationarity presented in Sec. 3 indicate that under some assumptions the time series can be considered as a stationary process. In the next sections, we will show that this hypothesis is not true. We find a point that divides examined data into two i.i.d. samples.

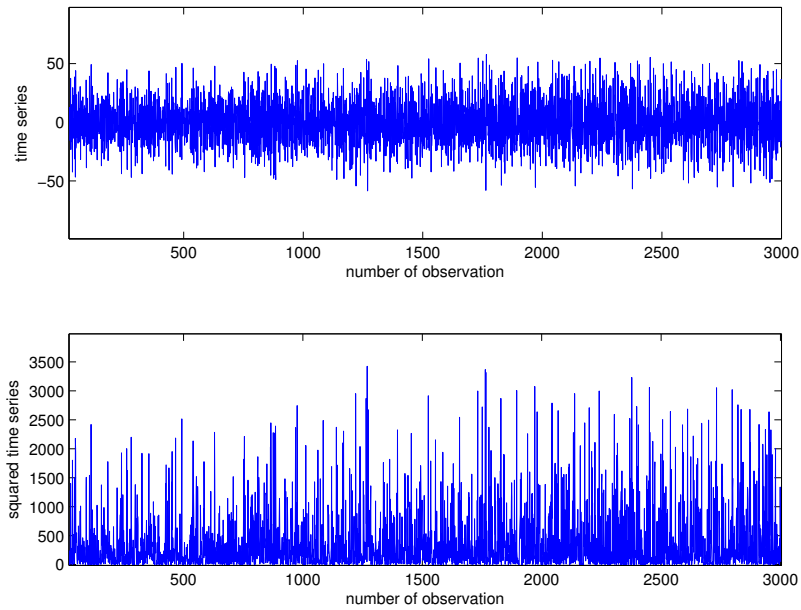

Fig. 2. The empirical time series from plasma physics that presents increments of floating potential fluctuations (in volts) of turbulent laboratory plasma for the small torus radial position $r = 9.8$ cm (top panel) and squared time series (bottom panel).

3. Statistical tests for stationarity

In order to make any inferences about the structure of a time series, we need some regularity over time in the behavior of the underlying series. This regularity can be formalized using a concept of stationarity, see [19]. We say that the time series is weakly stationary if the mean of the series is constant over time and the covariance between observations on time t and s depends only on their absolute difference $|s - t|$.

However, stationarity is not a common feature of time series and mostly we observe nonstationary behavior of the process. There are several types of nonstationarity. The trend nonstationarity means that the data posses some deterministic trend (for example, linear trend) but otherwise are stationary. This can easily be seen based on an autocorrelation function (for instance, a linear trend can be seen as a linear slow in time decay of autocorrelation function) [19]. The second type of nonstationarity is called difference nonstationarity, which means the process has to be differenced in order to become stationary. These two examples of nonstationarity are often encountered in real-life data. The class of unit-root tests helps to distinguish difference from trend nonstationarity. Under the null hypothesis that the

series is difference nonstationary, one can mention here Dickey–Fuller unit root tests [8–10] and Phillips–Perron unit root tests [11]. Testing in opposite direction, namely assuming that the time series is trend stationary against it is the difference nonstationary, one can apply the KPSS test provided by Kwiatkowski, Phillips, Schmidt and Shin [12].

The aforementioned types of nonstationarity can be successfully tested and recognized from the data but they are not the only problems which may be encountered during data analysis. Atypical observations, level shifts or variance change are common features of many real-life data sets [7, 20, 21]. Neglecting such effects may lead to inaccurate estimation of parameters of the model and in consequence inaccurate or a completely wrong prediction. Here, we discuss the effect of variance change in the data sets, thus there is no trend and differenced data have the same behavior as before differentiation. Such specific two-regimes time series was also considered in [16], where the following model for the innovations (independent sample) was considered

$$\epsilon_i' = \begin{cases} \epsilon_i & \text{if} \quad i < l\,, \\ \epsilon_i(1+\omega_{\mathrm{V}}) & \text{if} \quad i \geq l \end{cases} \tag{2}$$

for some point l, fixed number ω_{V} and under the assumption $\{\epsilon_i\}_{i=1}^n$ constitutes i.i.d. random variables from normal distribution. We can thus calculate the variance ratio of ϵ_i' before and after the structural change

$$\hat{r}_l = \frac{(l-1)\sum_{i=l}^n \epsilon_i'^2}{(n-l+1)\sum_{i=1}^{l-1}\epsilon_i'^2}\,, \tag{3}$$

where $(l-1)$ and $(n-l+1)$ are greater than zero. The variance ratio is an estimate of $(1+\omega_{\mathrm{V}})^2$ and is likelihood ratio test statistics of variance change under the assumption of normality. The test is the most powerful for step change in variance when the point l is known. If the critical point is unknown, one can apply variance ratio statistics to find it. In this case, we compute the variance ratio statistics for a stochastically independent series and obtain its minimum $\hat{r}_{\min}$ and maximum $\hat{r}_{\max}$ values

$$\hat{r}_{\min} = \min_{h\leq l\leq n-h}\{\hat{r}_l\}\,, \qquad \hat{r}_{\max} = \max_{h\leq l\leq n-h}\{\hat{r}_l\}\,,$$

where h is the positive integer denoting the minimum number of observations used to estimate the variance at the beginning and at the end of the sample. Then, we calculate

$$\hat{r} = \max\left\{\hat{r}_{\min}^{-1}, \hat{r}_{\max}\right\}\,.$$

The critical point l is the one at which $\hat{r}$ occurs.

The complete description of the procedure for detecting and adjusting the time series with two-regimes structure of type (2) is presented in [16]. Because the presented methodology is based on the assumption of normal distribution, which is a major disadvantage, therefore in the next section, we introduce the innovative procedure of estimation for the critical point that does not require any assumption of the distribution. This procedure is based on the behavior of the empirical second moment of the examined time series and is compatible with a two visual pre-tests for two-regimes structure.

4. Visual pre-tests for regime variance

In the first part of this section, we present two visual pre-tests that can confirm if the observed time series $X_1, X_2, \ldots, X_n$ constitutes a sample that satisfies relation (1). They are based on the behavior of the empirical second moment of the data. This approach was also proposed in [13] to test regime-variance behavior. But in contrast to [13], our methodology does not assume the Gaussian distribution of the underlying time series. In the first method, we propose to consider the following statistics

$$C_j = \sum_{i=1}^{j} X_i^2\,, \qquad j = 1, 2, \ldots, n\,. \tag{4}$$

If the random variables X and Y given in relation (1) have distributions with finite second moments σ_1^2 and σ_2^2, respectively, then the statistics C_j has the following property

$$E(C_j) = \begin{cases} j\sigma_1^2 & \text{for} \quad j \le l\,, \\ j\sigma_2^2 + l\left(\sigma_1^2 - \sigma_2^2\right) & \text{for} \quad j > l\,. \end{cases} \tag{5}$$

If $\sigma_1^2 = \sigma_2^2$, then the mean of C_j statistics is equal to $\sigma_1^2 j$ for all $j = 1, 2, \ldots, n$, therefore for i.i.d. sample, the expected value of the statistics is a linear function with the shift parameter equal to zero. This relation is not satisfied for distributions with infinite variances, but even in these cases significant changes in behavior of C_j statistics can be observed. Results of this pre-test are presented in Fig. 3 for different distributions of random variables X and Y in relation (1). Two cases, each consisting of three distributions are considered, namely pure Gaussian ($\mathcal{N}(\mu, \sigma)$), pure Lévy-stable ($\mathcal{S}(\alpha, \beta, \sigma, \mu)$), and Gaussian–Lévy-stable. In the first scenario, we consider the case when the parameters of distributions are close to each other and thus the structure change point is not easily visible (see left panel of Fig. 3). In the second scenario, we consider distributions with very different parameters, thus the critical point is observable in the simulated sample (the right panel of Fig. 3).

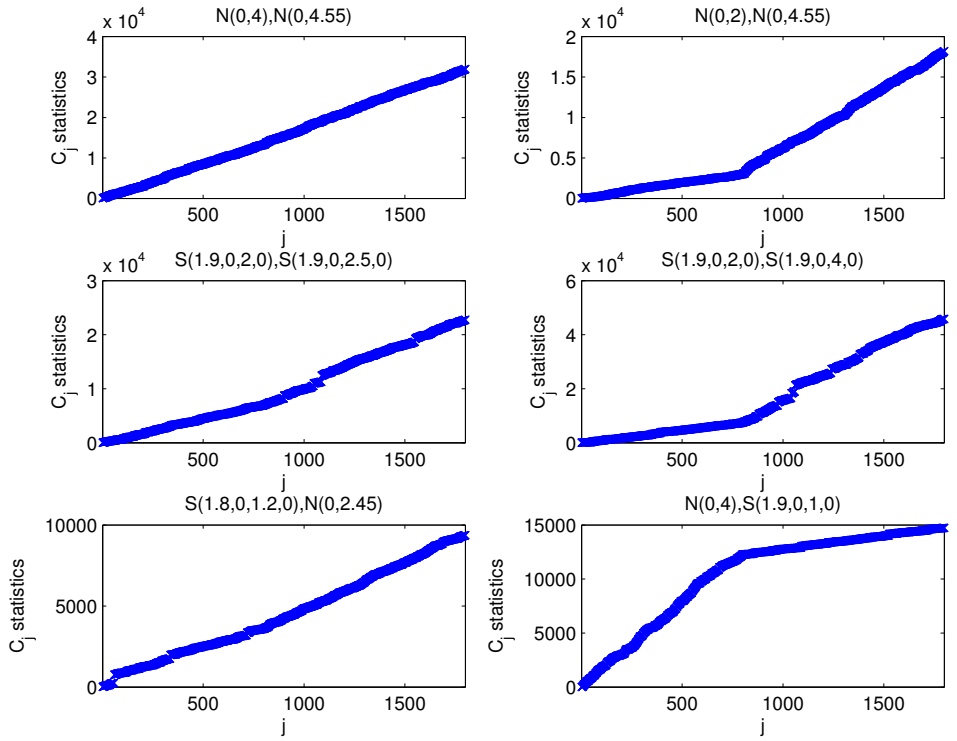

Fig. 3. The C_j statistics defined in (4) for two considered scenarios. In the left panel, we demonstrate results for cases when the parameters of distributions are close to each other (the first scenario). The right panel presents cases of distributions with very different parameters (the second scenario).

For the first scenario, we consider the following cases:

- the pure Gaussian case with $\mathcal{N}(0,4)$ and $\mathcal{N}(0,4.55)$ distribution for the first 800 and last 1000 observations, respectively,
- the pure Lévy-stable case with $\mathcal{S}(1.9,0,2,0)$ and $\mathcal{S}(1.9,0,2.5,0)$ distribution for the first 800 and last 1000 observations, respectively,
- the Lévy-stable-Gaussian case with $\mathcal{S}(1.8,0,1.2,0)$ and $\mathcal{N}(0,2.45)$ distribution for the first 800 and last 1000 observations, respectively.

In the second scenario, we consider following parameters of distributions:

- the pure Gaussian case with $\mathcal{N}(0,2)$ and $\mathcal{N}(0,4)$ distribution for first the 800 and last 1000 observations, respectively,

- the pure Lévy-stable case with $\mathcal{S}(1.9, 0, 2, 0)$ and $\mathcal{S}(1.9, 0, 4, 0)$ distribution for the first 800 and last 1000 observations, respectively,
- the Gaussian–Lévy-stable case with $\mathcal{N}(0, 4)$ and $\mathcal{S}(1.9, 0, 1, 0)$ distribution for the first 800 and last 1000 observations, respectively.

In the second visual pre-test, the behavior of the empirical second moment of the data from windows of width $k > 0$ was observed. The examined statistics has the following form

$$R_{j,k} = \sum_{i=j+1}^{j+k} X_i^2 \,, \qquad j = 0, 1, \ldots n - k \,, \tag{6}$$

where k is a given positive number called window width. We assume $k < l$. For finite variance distributions of X and Y, we can also calculate the ex-

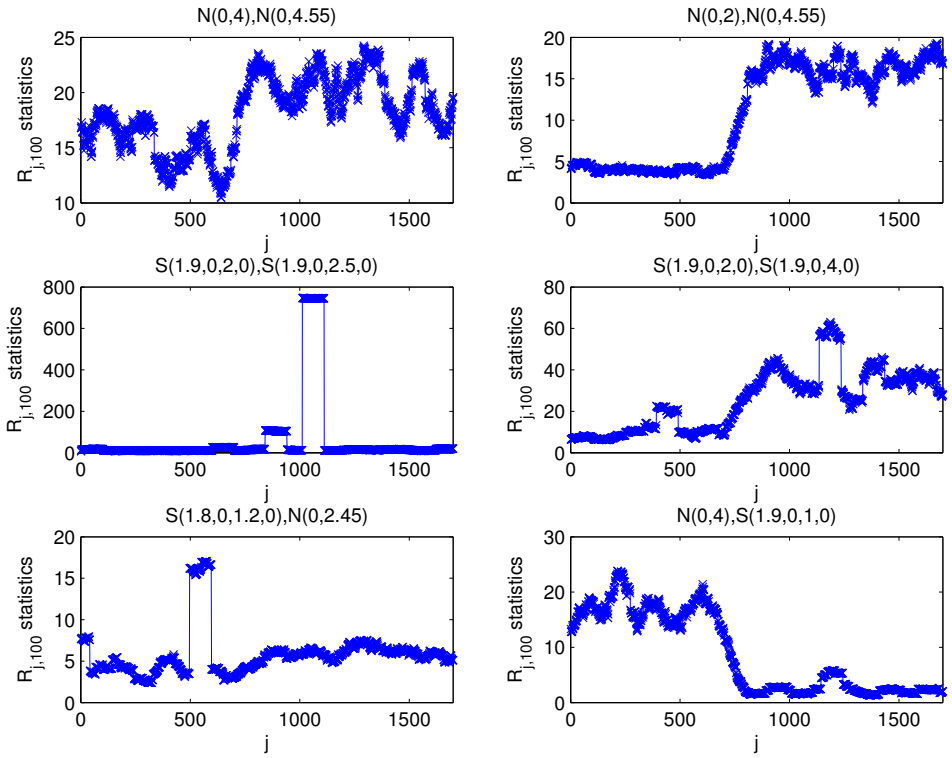

Fig. 4. The $R_{j,100}$ statistics defined in (6) for two considered scenarios. In the left panel, we demonstrate results for cases when the parameters of distributions are close to each other (the first scenario). The right panel presents cases of distributions with very different parameters (the second scenario).

pected value of $R_{j,k}$ statistic, namely $E(R_{j,k})$ is equal to

$$\begin{cases} k\sigma_1^2\,, & j+k \le l\,, \\ j\left(\sigma_2^2-\sigma_1^2\right)+l\left(\sigma_1^2-\sigma_2^2\right)+k\sigma_2^2\,, & j+1 \le l < j+k\,, \\ k\sigma_2^2\,, & j+1 > l\,, \end{cases} \tag{7}$$

where σ_1^2 and σ_2^2 are the second moments of the random variables X and Y, respectively. As we observe in (7), the mean of $R_{j,k}$ statistics for the given window width is constant when $j \le l-k$ or $j > l-1$. For $l-k < j \le l-1$, the statistics has a mean that is a linear function with respect to j. When X and Y have the same distributions, then the expected value of the statistics defined in (6) is constant for given k. The results of this pre-test are presented in Fig. 4, for two considered scenarios with different distributions presented above.

4.1. Estimation procedure for the critical point

In this part, we introduce the innovative method of estimating the critical point of change of the statistical properties in the sample that fulfills relation (1). The idea of the estimation procedure comes from the first visual pre-test described above. More precisely, we use the statistics C_j, $j=1,2,\ldots,n$ defined in (4) and its mean function $E(C_j)$ given in (5). The proposed method is an extension of that presented in [13], where the authors assume the Gaussian distribution of the examined data set. Moreover, in [13], the authors examine the asymptotic behavior of the investigated estimator, therefore, the results can be only useful for a large collection of data.

Our algorithm starts with dividing for the fixed $k=1,2,\ldots,n$ the C_j statistics into two sets $\{C_j : j=1,2,\ldots,k\}$ and $\{C_j : j=k+1,k+2,\ldots,n\}$. Next, we fit the linear regression lines $y_j^1(k) := a_1(k)j + b_1(k)$ and $y_j^2(k) := a_2(k)j + b_2(k)$ to the first and the second set, respectively. From ordinary regression theory, for such lines, the sums of squared distances $\sum_{j=1}^{k}(C_j - y_j^1(k))^2$ and $\sum_{j=k+1}^{n}(C_j - y_j^2(k))^2$ are minimized and, therefore, the line coefficients have the form, see [22]

$$\begin{aligned} a_1(k) &= \frac{\sum_{j=1}^{k} jC_j - \frac{(k+1)}{2}\sum_{j=1}^{k} C_j}{-\frac{1}{4}k(k+1)^2 + \frac{1}{6}k(k+1)(2k+1)}\,, \\ b_1(k) &= \frac{\frac{1}{3}(2k+1)\sum_{j=1}^{k} C_j - \sum_{j=1}^{k} jC_j}{-\frac{1}{2}k(k+1) + \frac{1}{3}k(2k+1)}\,. \end{aligned} \tag{8}$$

The coefficients $a_2(k)$, $b_2(k)$ have analogous formulas with summation from $j=k+1$ to n. Our estimator of the point l in relation (1) is defined as the

number k that minimalizes mentioned sums of squared distances

$$\hat{l} = \arg \min_{1 \le k \le n} \left[\sum_{j=1}^{k} \left(C_j - y_j^1(k) \right)^2 + \sum_{j=k+1}^{n} \left(C_j - y_j^2(k) \right)^2 \right]. \tag{9}$$

Let us stress that the proposed estimator $\hat{l}$ is invariant with respect to the sample distribution.

We compare the robustness of detecting the critical point of the underlying sample satisfying relation (1) with the method proposed in [16] and based on the variance ratio statistics given in (3). Let us remind that the variance ratio statistics is intended to detect the change point under the assumption of normal distribution of the examined series. The procedure is as follows: we simulate 1000 trajectories of length $n = 1800$ of stochastically independent random variables with the variance change point placed on 800th observation. Similar to the visual pre-tests, we consider two cases each consisting of three distributions. Details of the examined scenarios are presented above.

The results for the first scenario, where the critical point is not easily visible are presented in Fig. 5, where the first boxplot denotes results of $\hat{r}_l$ estimator presented in (3) while the second — is related to $\hat{l}$ estimator defined in (9). It can clearly be seen that estimator $\hat{l}$ is far more accurate than $\hat{r}_l$, even in the case of Gaussian distribution (see panel (a) in Fig. 5).

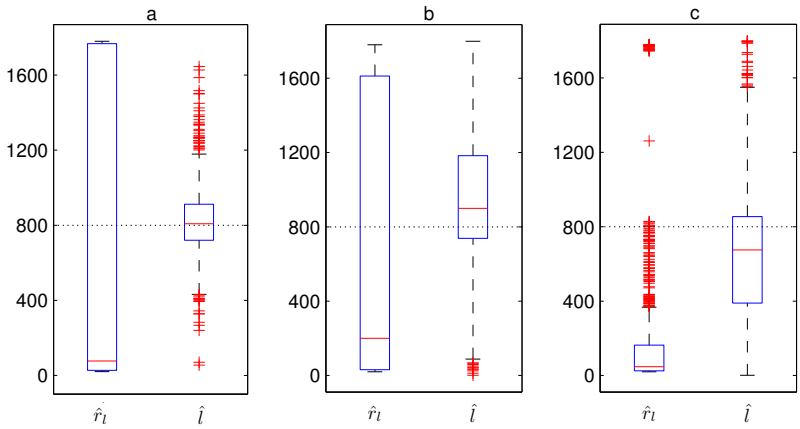

Fig. 5. Comparison of detection procedure for the critical variance change point for two estimators $\hat{r}_l$ and $\hat{l}$. Panel (a) $\mathcal{N}(0,4)$, $\mathcal{N}(0,4.55)$, panel (b) $\mathcal{S}(1.9,0,2,0)$, $\mathcal{S}(1.9,0,2.5,0)$, panel (c) $\mathcal{S}(1.8,0,1.2,0)$, $\mathcal{N}(0,2.45)$.

The results for the second scenario with a clear critical point are presented in Fig. 6. Also in this case it can be seen that $\hat{l}$ estimator performs better than $\hat{r}_l$.

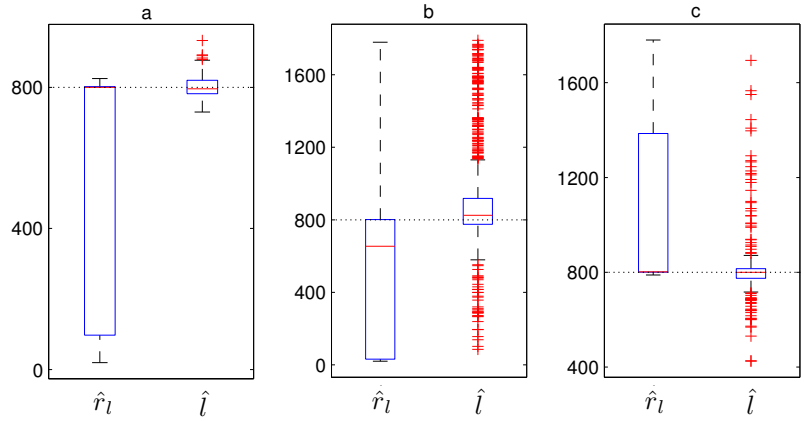

Fig. 6. Comparison of detection procedure for the critical variance change point for two estimators $\hat{r}_l$ and $\hat{l}$. Panel (a) $\mathcal{N}(0,2)$, $\mathcal{N}(0,4)$, panel (b) $\mathcal{S}(1.9,0,2,0)$, $\mathcal{S}(1.9,0,4,0)$, panel (c) $\mathcal{N}(0,4)$, $\mathcal{S}(1.9,0,1,0)$.

5. Statistical test for regime variance

In this section, we introduce the regime variance test that confirms our assumption of two-regimes behavior given in relation (1). It also confirms the preliminary results obtained by using the visual pre-tests presented in the previous section.

The procedure is based on the analysis of the empirical second moment of a given sample. Let us point out that it can be used for distributions with a theoretical second moment but also for those with an infinite one. Even in this case, the theoretical second moment exists. Moreover, the test is based on the quantiles that without assumption of the distribution we can determine on the basis of the empirical distribution function, therefore, we extend the methodology presented in [13].

The $\mathcal{H}_0$ hypothesis is defined as follows: observed time series does not satisfy relation (1), this means the quantiles of the squared series do not change in time. The hypothesis is satisfied in the case of i.i.d. random variables but also when the distributions of two parts (divided by point l) are different but quantiles $q_{\alpha/2}$ and $q_{1-\alpha/2}$ of the squared data are at the same level.

The $\mathcal{H}_1$ hypothesis is formulated as: observed time series has at least the representation (1), *i.e.* there are at least two regimes of the data for which the appropriate quantiles of the squared time series are different. Let us point out that the $\mathcal{H}_0$ hypothesis will be rejected when the squared series has more than two regimes.

The testing of regime variance is based on the assumption the real data constitutes a sample of independent variables, therefore, before testing we have to confirm that the given sample constitutes independent data. We propose here to use the simple visual method based on the autocorrelation function (ACF). For an independent sample, the ACF is close to zero for all lags greater than zero. Basic properties of this methodology can be found in [23].

The procedure of **regime variance testing** for given time series X_1, $X_2, \ldots, X_n$ proceeds as follows:

1. Determine the critical point l according to the procedure presented in Sec. 4. Let us emphasize that also under $\mathcal{H}_0$ hypothesis, the l point exists and is between 1 and n.

2. Divide the squared time series into two vectors: $\boldsymbol{W}_1 = [X_1^2, ..., X_l^2]$ and $\boldsymbol{W}_2 = [X_{l+1}^2, ..., X_n^2]$. Find empirical standard deviations $\hat{\sigma}_1$ and $\hat{\sigma}_2$ of $\boldsymbol{W}_1$ and $\boldsymbol{W}_2$, respectively. For simplicity, let us assume that $\hat{\sigma}_1 < \hat{\sigma}_2$. In the case of distribution without theoretical second moment, the empirical standard deviation exists and can be calculated on the basis of the observed data.

3. Construct quantiles from the distribution of the squared time series from the vector $\boldsymbol{W}_1$ (for that the empirical standard deviation was smaller), *i.e.* numbers $q_{\alpha/2}$ and $q_{1-\alpha/2}$ that satisfy the relation

$$P\left(q_{\alpha/2} < X_i^2 < q_{1-\alpha/2}\right) = 1 - \alpha\,, \qquad \text{for each} \quad i = 1, 2, \ldots, l\,,$$

   where α is a given confidence level. Under the $\mathcal{H}_0$ hypothesis without the assumption of the distribution, the appropriate quantiles can be determined on the basis of the empirical cumulative distribution function. Because $X_{l+1}^2, X_2^2, \ldots, X_n^2$ are independent, therefore, the statistics B has a binomial distribution with parameters $n-l$ and $p = 1-\alpha$. Therefore, the p-value of the test we calculate as $P(Z < B)$, where Z has binomial distribution with $(n-l, p)$ parameters.

4. If the calculated p-value is greater than the α parameter, then we accept the $\mathcal{H}_0$ hypothesis. Otherwise, if the calculated p-value is smaller than the α parameter, then we reject the $\mathcal{H}_0$ hypothesis and accept $\mathcal{H}_1$.

The complementary part of this section is an examination of the performance of estimator (9) and the variance regime test described above via the Monte Carlo method. First, the first order error for our test is checked, *i.e.* the rejection of a true $\mathcal{H}_0$ hypothesis. For this purpose, we generate 1000 trajectories of length 1800 of stochastically independent random variables for each of three cases:

- the Gaussian case with $\mathcal{N}(0,2)$ distribution,
- the Lévy-stable case with $\mathcal{S}(1.8,0,1,0)$ distribution,
- the Gaussian–Lévy-stable case with $\mathcal{N}(0,1)$ and $\mathcal{S}(1.9,0,1,0)$ distribution for each half of the sample, randomly permuted.

In our simulations, the significance level $\alpha = 0.05$ and the unknown distribution of samples are assumed. Therefore, in the testing procedure the empirical quantiles are applied. We note that the first two cases (pure Gaussian and Lévy-stable) are the special simplified versions of $\mathcal{H}_0$, *i.e.* i.i.d. data. Obviously, the constancy of theoretical quantiles $q_{\alpha/2}$ and $q_{1-\alpha/2}$ implies the closeness between the empirical versions computed in the testing algorithm. The Gaussian–Lévy-stable case concerns two different distributions of data changing dynamically (randomly permuted) in the time domain. Therefore, it is in contrast to the $\mathcal{H}_1$ hypothesis, where different distributions are concentrated in two disjointed time intervals.

The results of the conducted simulations are presented in Table I. For the testing procedure, we apply the sample mean value of obtained estimators $\hat{l}$ from each generated sample. That mean value of $\hat{l}$ is 881.37, 916.34 and 104.31 for each of the three considered cases, respectively. They are close to half of the sample length, which is quite intuitive for data satisfying $\mathcal{H}_0$. We see that a large number of times the test correctly does not reject the true null hypothesis $\mathcal{H}_0$ and the error of the first order is strongly rare, see the $\mathcal{H}_1$-column. Moreover, the p-values corresponding to the acceptance of $\mathcal{H}_0$

TABLE I

Numbers of correct accepting (with mean p-value) and incorrect rejecting the true $\mathcal{H}_0$.

Distribution of samples	$\mathcal{H}_0$	p-value	$\mathcal{H}_1$
$\mathcal{N}(0,2)$	866	0.5623	134
$\mathcal{S}(1.8,0,1,0)$	865	0.5349	135
$\mathcal{N}(0,2)$, $\mathcal{S}(1.9,0,1,0)$	889	0.5621	111

are rightly higher than significance level $\alpha = 0.05$, see Fig. 7. The column of Table I with p-value contains the mean of such p-values. Moreover, in the $\mathcal{H}_0$-column and $\mathcal{H}_1$-column, the numbers of correct accepting and incorrect rejecting $\mathcal{H}_0$ are presented respectively. Our next task is to explore the statistical power of the examined test. This is equivalent to investigating the error of the second order, *i.e.* accepting a false $\mathcal{H}_0$ hypothesis. In order to calculate the error of the second order, 1000 trajectories of length 1800 of stochastically independent random variables are simulated for each of the three cases from the first scenario described in Sec. 4 satisfying the $\mathcal{H}_1$ hypothesis.

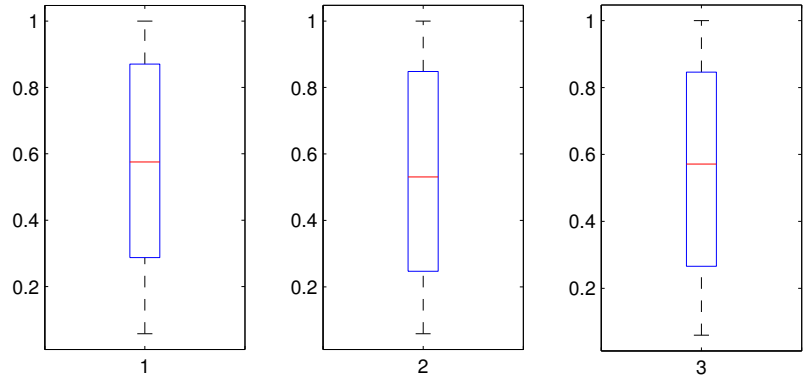

Fig. 7. The boxplots of p-values corresponding to the correct accepting of true $\mathcal{H}_0$: (1) $\mathcal{N}(0, 2)$, (2) $\mathcal{S}(1.8, 0, 1, 0)$, (3) permuted $\mathcal{N}(0, 1)$, $\mathcal{S}(1.9, 0, 1, 0)$.

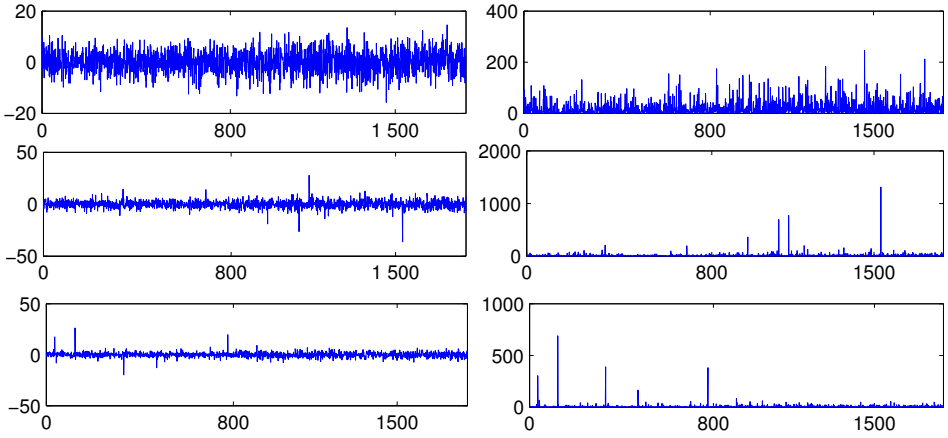

Fig. 8. The exemplary samples (left panels) and squared samples (right panels) for three considered cases of $\mathcal{H}_1$: (1) $\mathcal{N}(0, 4)$, $\mathcal{N}(0, 4.55)$, (2) $\mathcal{S}(1.9, 0, 2, 0)$, $\mathcal{S}(1.9, 0, 2.5, 0)$, (3) $\mathcal{S}(1.8, 0, 1.2, 0)$, $\mathcal{N}(0, 2.45)$.

In all three cases, the differences of distribution parameters are quite small and the $\mathcal{H}_1$ hypothesis statement can be invisible from the data or its squares, see Fig. 8. This means that the efficiency of the proposed test in a very sophisticated cases is checked.

We apply the estimator (9) and adopt the regime variance test assuming the unknown data distribution. The results of the conducted simulations with significant level $\alpha = 0.05$ are presented in Table II. For the testing procedure, the sample mean value of obtained estimators $\hat{l}$ from each generated sample is applied. The mean value of $\hat{l}$ is 822.28, 943.72 and 646.42 for each of the three considered cases from the first scenario, respectively. We see that more times the test correctly rejects the false null hypothesis $\mathcal{H}_0$ and the error of the second order is rare, see the $\mathcal{H}_0$-column. The worst result was obtained in the third case with different distributions. However, the p-values corresponding to the rejection of $\mathcal{H}_0$ are rightly lower than the significance level $\alpha = 0.05$, see Fig. 9. The column of Table II with p-value contains the mean of such p-values. Moreover, in the $\mathcal{H}_0$-column and $\mathcal{H}_1$-column the

TABLE II

Numbers of correct rejecting (with mean p-value) and incorrect accepting the false $\mathcal{H}_0$.

Distribution of samples	$\mathcal{H}_1$	p-value	$\mathcal{H}_0$
$\mathcal{N}(0,4)$, $\mathcal{N}(0,4.55)$	759	0.0061	241
$\mathcal{S}(1.9,0,2,0)$, $\mathcal{S}(1.9,0,2.5,0)$	758	0.0054	242
$\mathcal{S}(1.8,0,1.2,0)$, $\mathcal{N}(0,2.45)$	652	0.0044	348

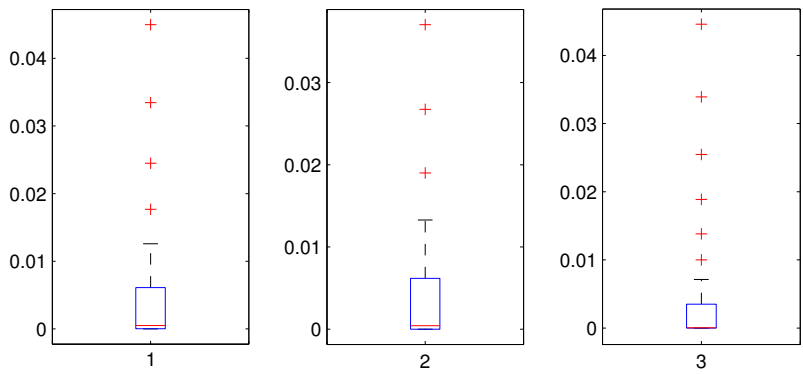

Fig. 9. The boxplots of p-values corresponding to the correct rejecting of false $\mathcal{H}_0$: (1) $\mathcal{N}(0,4)$, $\mathcal{N}(0,4.55)$, (2) $\mathcal{S}(1.9,0,2,0)$, $\mathcal{S}(1.9,0,2.5,0)$, (3) $\mathcal{S}(1.8,0,1.2,0)$, $\mathcal{N}(0,2.45)$.

numbers of incorrect accepting $\mathcal{H}_0$ and correct accepting $\mathcal{H}_1$ (the power of the test), are presented respectively. We also strongly stress that from the construction of the studied test, the rejection of $\mathcal{H}_0$ hypothesis is equivalent to the acceptance of $\mathcal{H}_1$. In other words, the rejection of $\mathcal{H}_0$ is only possible when $\mathcal{H}_1$ is true or in the case of first order error.

6. Plasma data analysis

In this section, the real data sets presented in Figs. 1 and 2 are analyzed by using the tests for regime variance described in Secs. 4 and 5. In Fig. 10, we demonstrate the results of the visual pre-tests for increments of floating potential fluctuations of turbulent laboratory plasma for the small torus radial position $r = 9.7$ cm (corresponding to Fig. 1).

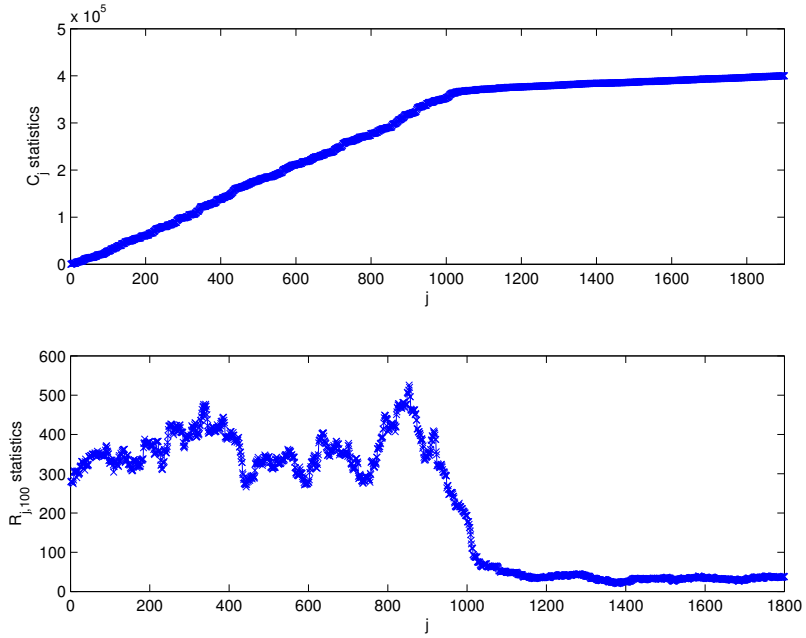

Fig. 10. The visual pre-tests for regimes variance of time series that presents increments of floating potential fluctuations of turbulent laboratory plasma for the small torus radial position $r = 9.7$ cm.

As can be observed, the visual pre-tests indicate the behavior formulated in (1). Moreover, the critical point l, that divides the time series into two independent samples with appropriate statistical properties that do not change over time can also be determined. The critical point is estimated by using the procedure described in Sec. 4 and the result is 1055. In the next step of our analysis, the $\mathcal{H}_0$ hypothesis is tested, *i.e.* the hypothesis that the

squared time series has quantiles that do not change over time. According to the procedure presented in Sec. 5, first independence is confirmed by using ACF function, see Fig. 11.

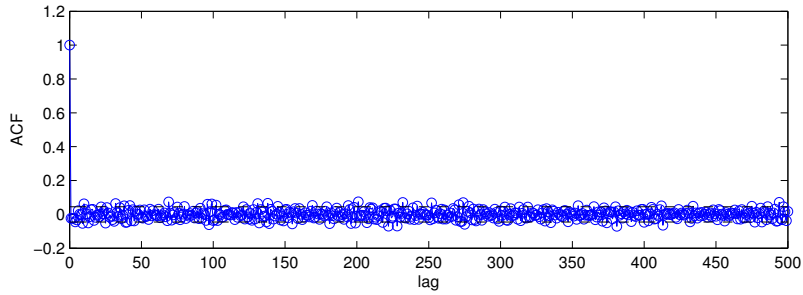

Fig. 11. ACF of the time series that presents increments of floating potential fluctuations of turbulent laboratory plasma for the small torus radial position $r = 9.7$ cm. Such behavior of autocorrelation function suggests that the data can be considered as independent sample.

The regime variance test confirms that the examined data set has at least two regimes, *i.e.* it has representation (1). This is related to the fact that with a confidence level $\alpha = 0.05$, the obtained p-value is equal to 0.0425 (we reject $\mathcal{H}_0$). Because we have estimated the critical point l, that divides the analyzed time series into two parts, we can examine if the separate vectors can be considered as independent samples with the same appropriate quantiles of squared data. In order to do this, we use the regime variance test once again for samples $X_1, \ldots, X_{1055}$ and $X_{1056}, \ldots, X_{1900}$. For the first time series, the test returns p-value at the level 0.5967, which indicates we can assume the squared data have appropriate quantiles that do not change over time. If we test the second part of the data set, namely observations from 1056 to 1900, we get a p-value equal to 0.9829, therefore, also for this vector we can conclude that appropriate statistical properties do not change. Moreover, if we assume the data from two considered parts constitute i.i.d. samples (that is one of the possibilities when $\mathcal{H}_0$ hypothesis is satisfied), we can test the distributions. By using tests based on the empirical cumulative distribution function completely described in [14], we conclude the observations $X_1, \ldots, X_{1055}$ come from the Lévy–stable distribution with a stable parameter equal to 1.76 and $\sigma = 12.14$, while the data $X_{1056}, \ldots, X_{1900}$ have the Lévy-stable distribution with parameters $\alpha = 1.91$ and $\sigma = 4.2$. For both samples, we use McCulloch's estimation method, [24].

As we have mentioned in Sec. 2, the testing procedure can also be used for data for which the critical point l is not as visible as in the previous case, see Fig. 2. In Fig. 12, the results of the visual pre-tests described in Sec. 4 are

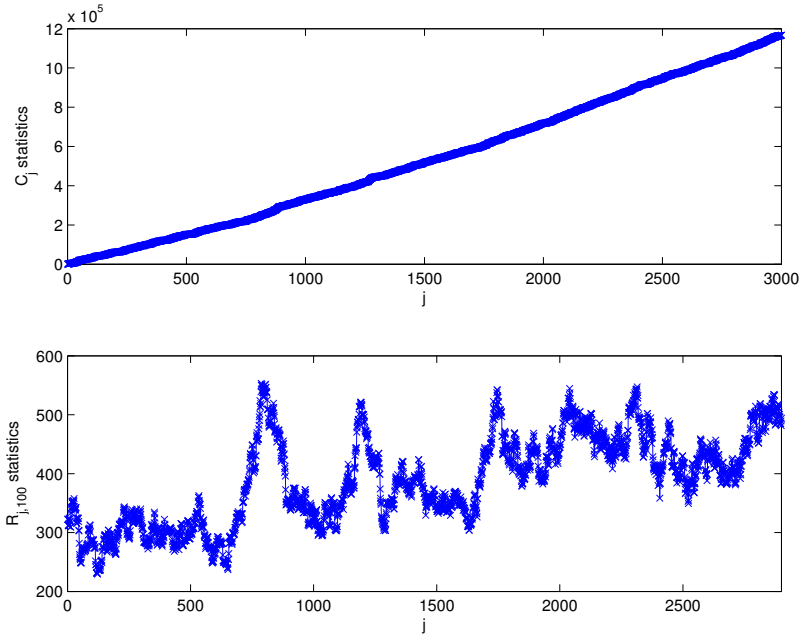

Fig. 12. The visual pre-tests for regimes variance of time series that presents increments of floating potential fluctuations of turbulent laboratory plasma for the small torus radial position $r = 9.8$ cm.

presented for data that describes increments of floating potential fluctuations of turbulent laboratory plasma for the small torus radial position $r = 9.8$ cm. As can be observed, on the basis of the behavior of C_j and $R_{j,k}$, statistics defined in (4) and (6), respectively, we cannot conclude that the data set exhibits the behavior described in (1). But the procedure of estimating the critical point returns to 1763. According to the scheme of regime variance testing presented in Sec. 5, in the first step independence of the time series is confirmed. The plot of ACF is presented in Fig. 13.

Next, we can test if the hypothesis $\mathcal{H}_0$ is satisfied for the time series presented in Fig. 2. The obtained p-value equal to 0.0011 indicates the data has at least two regimes with different statistical properties. Similarly, as for the first data set, the time series can be divided into two separate vectors and tested if we can consider them as samples for which the characteristics do not change with respect to time. For the first part, namely data from 1 to 1763, we get p-value at the level 0.593, while for the second vector (*i.e.* observations form 1764 to 3000) the p-vale is equal to 0.591. These results indicate that two considered vectors do not satisfy relation (1) and can be considered as i.i.d. samples. Under this assumption, we test the distributions and obtain the two considered parts come from the Lévy-stable distribution.

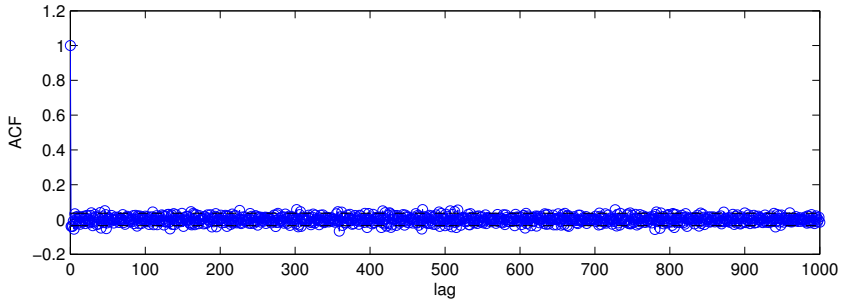

Fig. 13. ACF of the time series that presents increments of floating potential fluctuations of turbulent laboratory plasma for the small torus radial position $r = 9.8$ cm. Such behavior of autocorrelation function suggests that the data can be considered as independent sample.

For the first vector, the following estimates of the parameters are obtained: $\alpha = 1.9484$ and $\sigma = 12.9505$, while the estimated values of the parameters for the vector containing observations $X_{1764}, \ldots, X_{3000}$ are: $\alpha = 1.7983$ and $\sigma = 14.1099$.

7. Conclusions

In this paper, we have examined time series that exhibit two-regimes behavior. We have introduced a new estimation procedure for the recognition of the critical point that divides the observed time series into two regimes with different statistical properties expressed in the language of the quantiles for squared data (Sec. 4). We have also developed three tests that can confirm our assumption of two-regimes behavior (Secs. 4 and 5). The universality of the presented methodology comes from the fact that it does not assume the distribution of the examined time series, therefore, it can be applied to a rich class of real data sets. We extend the methodology presented in the literature, where the assumption of Gaussian distribution is required. The theoretical results we have illustrated using the simulated time series and analysis of two real data sets related to turbulent laboratory plasma.

The J.G. and G.S. would like to acknowledge that their research is co-financed by the European Union as part of the European Social Fund.

REFERENCES

[1] J.M. Sarabia, F. Prieto, *Physica A* **388**, 4179 (2009).

[2] P. Repetowicz, P. Richmond, *Acta Phys. Pol. B* **36**, 2785 (2005).

[3] R. Weron, in: *Handbook of Computational Statistics: Concepts and Methods*, eds. J.E. Gentle, W. Haerdle, Y. Mori, Springer, Berlin 2004.

[4] K. Burnecki, J. Gajda, G. Sikora, *Physica A* **390**, 3136 (2011).

[5] J. Janczura, S. Orzeł, A. Wyłomańska, *Physica A* **390**, 4379 (2011).

[6] K. Burnecki, A. Weron, *Phys. Rev.* **E82**, 021130 (2010).

[7] I.H. Gencn, M. Arzaghi, *J. Franklin Inst.* **348**, 1615 (2011).

[8] D. Dickey, W. Fuller, *J. Am. Statist. Assoc.* **74**, 427 (1979).

[9] D. Dickey, W. Fuller, *Econometrica* **49**, 1057 (1981).

[10] S.E. Said, D. Dickey, *Biometrika* **71**, 599 (1984).

[11] P.C.B. Phillips, P. Perron, *Biometrika* **75**, 335 (1988).

[12] D. Kwiatkowski, P.C.B. Phillips, P. Schmidt, Y. Shin, *J. Econometrics* **54**, 159 (1992).

[13] C. Inclan, G.C. Tiao, *J. Am. Statist. Assoc.* **89**, 913 (1994).

[14] K. Burnecki *et al.*, *Phys. Rev.* **E85**, 056711 (2012).

[15] A. Wyłomańska, *Acta Phys. Pol. B* **43**, 1241 (2012).

[16] R.S. Tsay, *J. Forecasting* **7**, 1 (1988).

[17] V.Yu. Gonchar *et al.*, *Plasma Phys. Rep.* **29**, 380 (2003).

[18] F. Wagner, *Plasma Phys. Control. Fusion* **49**, B1 (2007).

[19] J.D. Cryer, K.-S. Chan, *Time Series Analysis with Applications in R*, second edition, Springer, New York 2008.

[20] G.C. Chow, *Econometrica* **28**, 591 (1960).

[21] R.E. Quandt, *J. Am. Statist. Assoc.* **55**, 324 (1960).

[22] N.R. Draper, H. Smith, *Applied Regression Analysis*, Wiley Series in Probability and Statistics, 1988.

[23] M.B. Priestley, *Spectral Analysis and Time Series*, Academic Press, London, 1982.

[24] J.H. McCulloch, *Commun. Statist. — Simul. Comput.* **15**, 1109 (1986).